

Online appendices are unedited and posted as supplied by the authors.

Supplemental table 1. Acquisition parameters of multimodal MRI

Sequence	Basic	TR/TE	FOV	Slice thickness	Gap	Matrix	b-value	Others
3D-T1WI	TSE	2300/2.27	250×250	1	0.5	256×256	-	-
T2WI	TSE	6610/96	230×208	3	0.9	448×313	-	-
DWI	EPI	5000/78	230×230	5	1.5	256×256	1000	-
DTI	EPI	9100/100	245×245	2	0.6	224×224	1000	Thirty diffusion gradient directions
rs-fMRI	EPI	2800/30	220×220	3.2	0.8	64 × 64	-	In-plane resolution= 3.4×3.4×3.2mm

Note: MRI:magnetic resonance imaging; DWI: diffusion weight imaging; DTI: diffusion tensor imaging; rs-fMRI: resting-state functional magnetic resonance imaging; TSE: fast spin echo; EPI: echo planar Imaging; TR: repetition time, millisecond (ms); TE: echo time, ms; FOV: field of view, millimeter² (mm²);Slice thickness: mm, Gap: mm.

Supplemental table 2. The univariate analysis of structural connectivity^a between stroke patients and healthy control.

Brain structure	MD					FA				
	Stroke		Healthy control		P	Stroke		Healthy control		P
	Mean	SD	Mean	SD		Mean	SD	Mean	SD	
MCP	0.74	0.05	0.71	0.04	0.018	0.57	0.03	0.58	0.02	0.054
PCT	0.78	0.12	0.76	0.10	0.430	0.50	0.07	0.52	0.05	0.118
GCC	0.84	0.09	0.76	0.04	0.000	0.59	0.05	0.64	0.02	0.000
BCC	0.98	0.26	0.84	0.08	0.016	0.58	0.09	0.65	0.05	0.001
SCC	0.97	0.27	0.84	0.06	0.034	0.64	0.10	0.69	0.03	0.039
FX	1.65	0.34	1.50	0.33	0.077	0.46	0.10	0.51	0.09	0.018
CST-R	0.76	0.07	0.74	0.08	0.282	0.57	0.06	0.59	0.05	0.120
CST-L	0.77	0.09	0.74	0.07	0.166	0.57	0.07	0.60	0.04	0.113
ML-R	0.77	0.08	0.74	0.04	0.136	0.61	0.07	0.63	0.03	0.261
ML-L	0.77	0.09	0.74	0.04	0.151	0.61	0.07	0.62	0.03	0.561
ICP-R	0.76	0.07	0.73	0.02	0.027	0.57	0.05	0.59	0.02	0.068
ICP-L	0.78	0.11	0.73	0.02	0.035	0.57	0.06	0.59	0.02	0.074
SCP-R	0.96	0.10	0.93	0.08	0.175	0.68	0.06	0.68	0.03	0.698
SCP-L	0.96	0.09	0.92	0.08	0.054	0.68	0.07	0.69	0.02	0.300
CP-R	0.81	0.14	0.73	0.06	0.012	0.65	0.05	0.67	0.03	0.054

DOI: 10.1503/jpn240084

Online appendices are unedited and posted as supplied by the authors.

CP-L	0.81	0.19	0.73	0.06	0.047	0.65	0.07	0.68	0.02	0.045
ALIC-R	0.77	0.07	0.71	0.07	0.001	0.54	0.05	0.58	0.03	0.000
ALIC-L	0.78	0.10	0.71	0.07	0.002	0.51	0.06	0.55	0.04	0.001
PLIC-R	0.72	0.04	0.68	0.03	0.000	0.65	0.04	0.67	0.02	0.026
PLIC-L	0.72	0.05	0.70	0.04	0.063	0.65	0.04	0.67	0.02	0.077
RLIC-R	0.83	0.18	0.74	0.03	0.034	0.59	0.06	0.62	0.03	0.055
RLIC-L	0.80	0.11	0.75	0.03	0.031	0.61	0.06	0.64	0.02	0.044
ACR-R	0.82	0.10	0.75	0.09	0.009	0.42	0.05	0.47	0.04	0.000
ACR-L	0.82	0.11	0.75	0.10	0.009	0.41	0.05	0.45	0.04	0.000
SCR-R	0.80	0.15	0.70	0.08	0.007	0.48	0.05	0.52	0.04	0.002
SCR-L	0.81	0.16	0.73	0.12	0.042	0.48	0.05	0.51	0.05	0.018
PCR-R	0.90	0.19	0.81	0.12	0.047	0.46	0.05	0.49	0.04	0.052
PCR-L	0.91	0.24	0.80	0.13	0.070	0.45	0.06	0.48	0.05	0.036
PTR-R	0.88	0.16	0.82	0.05	0.078	0.57	0.07	0.60	0.04	0.053
PTR-L	0.90	0.16	0.83	0.05	0.063	0.58	0.06	0.60	0.04	0.039
SS-R	0.89	0.25	0.81	0.04	0.164	0.54	0.07	0.58	0.03	0.055
SS-L	0.88	0.13	0.84	0.05	0.156	0.55	0.05	0.57	0.03	0.092
EC-R	0.80	0.08	0.75	0.05	0.007	0.45	0.04	0.47	0.03	0.009
EC-L	0.81	0.09	0.76	0.07	0.015	0.45	0.05	0.48	0.04	0.011
CGC-R	0.77	0.18	0.72	0.04	0.216	0.49	0.05	0.53	0.03	0.002
CGC-L	0.79	0.22	0.73	0.03	0.219	0.50	0.06	0.54	0.03	0.005
CGH-R	0.81	0.13	0.76	0.04	0.072	0.48	0.05	0.51	0.04	0.018
CGH-L	0.84	0.18	0.77	0.03	0.081	0.48	0.04	0.51	0.04	0.005
FX/ST-R	1.06	0.20	0.93	0.08	0.005	0.51	0.06	0.56	0.04	0.001
FX/ST-L	0.87	0.10	0.81	0.05	0.013	0.55	0.05	0.58	0.04	0.006
SLF-R	0.76	0.07	0.70	0.04	0.000	0.49	0.05	0.53	0.03	0.008
SLF-L	0.76	0.10	0.70	0.04	0.011	0.48	0.06	0.52	0.03	0.008
SFO-R	0.84	0.18	0.73	0.10	0.006	0.45	0.08	0.52	0.04	0.000
SFO-L	0.89	0.17	0.77	0.14	0.004	0.42	0.07	0.48	0.05	0.000
IFO-R	0.80	0.05	0.77	0.04	0.019	0.54	0.04	0.57	0.03	0.001
IFO-L	0.80	0.06	0.77	0.04	0.006	0.51	0.05	0.54	0.03	0.007

DOI: 10.1503/jpn240084

Online appendices are unedited and posted as supplied by the authors.

UNC-R	0.77	0.04	0.76	0.04	0.258	0.53	0.05	0.54	0.04	0.334
UNC-L	0.78	0.11	0.75	0.04	0.261	0.52	0.06	0.54	0.04	0.260
TAP-R	1.74	0.32	1.45	0.23	0.000	0.41	0.09	0.50	0.07	0.000
TAP-L	1.93	0.33	1.66	0.26	0.001	0.37	0.08	0.45	0.08	0.000

Note: ^a Mean (SD), ANOVA. MD: mean diffusivity, L: left, R: right, MCP: middle cerebellar peduncle, PCT: pontine crossing tract (part of the MCP); GCC: genu of the corpus callosum, BCC: body of the corpus callosum, SCC: splenium of the corpus callosum, FX: fornix, CST: corticospinal tract, ML: medial lemniscus, ICP: inferior cerebellar peduncle, SCP: superior cerebellar peduncle, CP: cerebral peduncle, ALIC: anterior limb of the internal capsule, PLIC: posterior limb of the internal capsule, RLIC: retrolenticular part of internal capsule, ACR: anterior corona radiata, SCR: superior corona radiata, PCR: posterior corona radiata, PTR: posterior thalamic radiation (including optic radiation), SS: sagittal stratum (including inferior longitudinal fasciculus and inferior fronto-occipital fasciculus), EC: external capsule, CGC: cingulum (cingulate gyrus), CGH: cingulum (hippocampus), FX/ST: fornix (cres) / stria terminalis (can not be resolved with current resolution), SLF: superior longitudinal fasciculus, SFO: superior fronto-occipital fasciculus (could be a part of the anterior internal capsule), IFO: inferior fronto-occipital fasciculus, UNC: uncinata fasciculus, TAP: tapetum.

Supplemental table 3. The collinearity between the putative risk factors following the correlation analysis.

Variable 1	Varibale 2	r	P
L-occipital atrophy	R-cingulate	0.446	.000
L-temporal atrophy	FX-FA	-0.425	.000
BCC-FA	R-TAP--FA	0.612	.000
FX-FA	FX-MD	-0.929	.000
L-SFO-FA	R-TAP--FA	0.504	.000
L-UNC-FA	BBC-FA	0.408	.000
R-TAP-MD	L-TAP-MD	0.8	.000
R-TAP-MD	BBC-FA	-0.445	.000

Note: L: left, R:

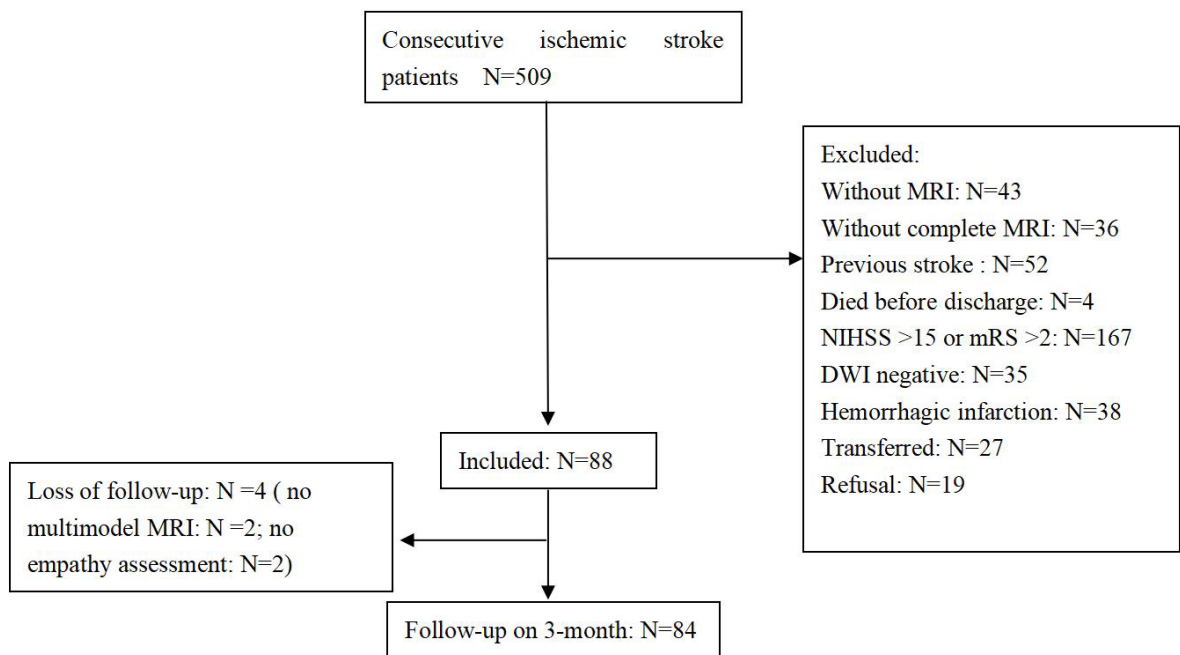
right, FA: fractional anisotropy, MD: mean diffusivity, BCC: body of the corpus callosum,

DOI: 10.1503/jpn240084

Online appendices are unedited and posted as supplied by the authors.

FX: fornix, SFO: superior fronto-occipital fasciculus, UNC: uncinate fasciculus, TAP: tapetum.

Figure 1 Flow-chart



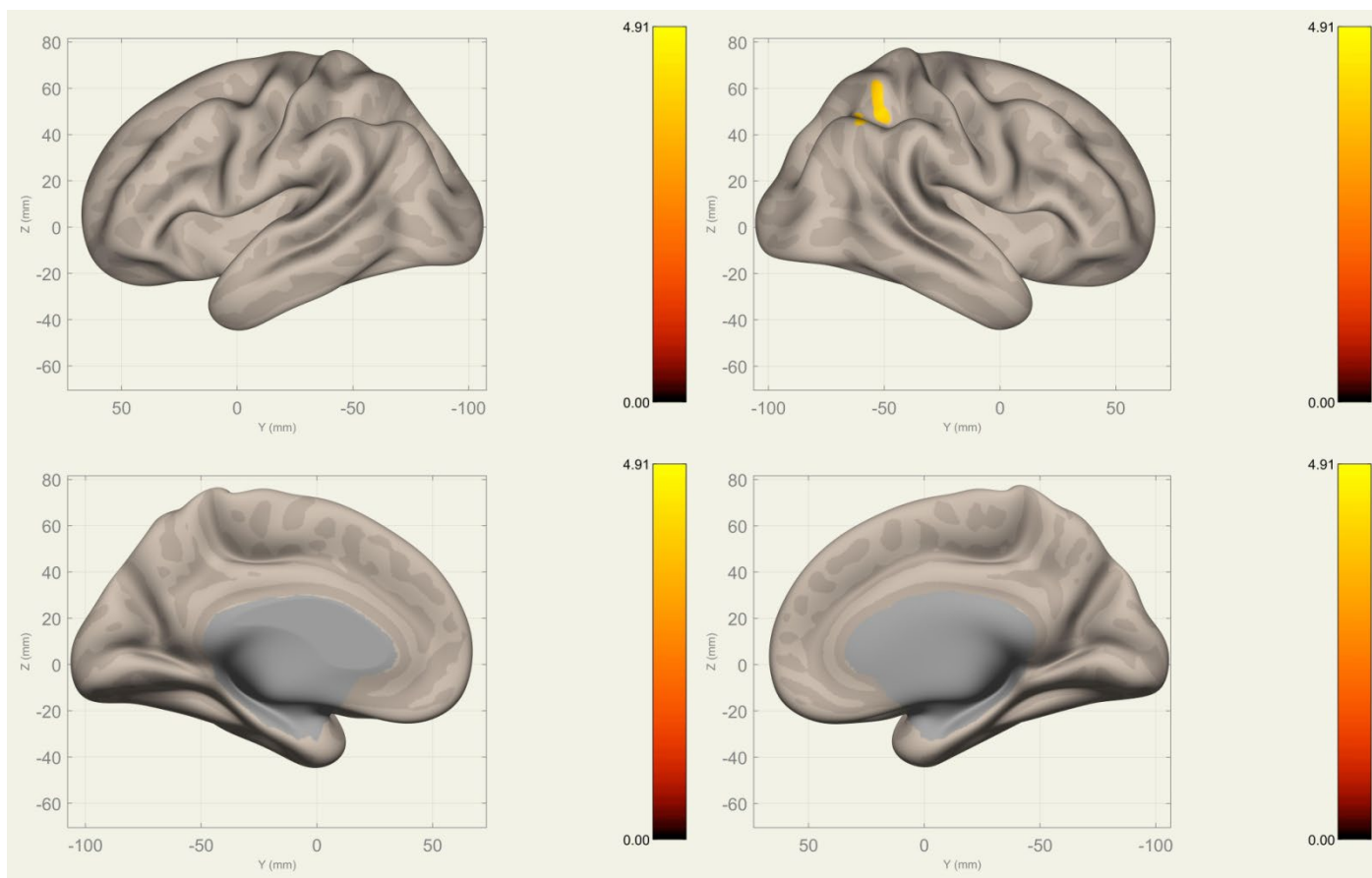
Supplemental figure 1. Flowchart of the study.

Appendix 2 to Qu J-F, Liu X-W, Wang M-Z, et al. Structural-informed functional MRI analysis of patients with empathy impairment following stroke. *J Psychiatry Neurosci* 2024. Copyright © 2024 The Author(s) or their employer(s).

To receive this resource in an accessible format, please contact us at cmaigroup@cmaj.ca.

DOI: 10.1503/jpn240084

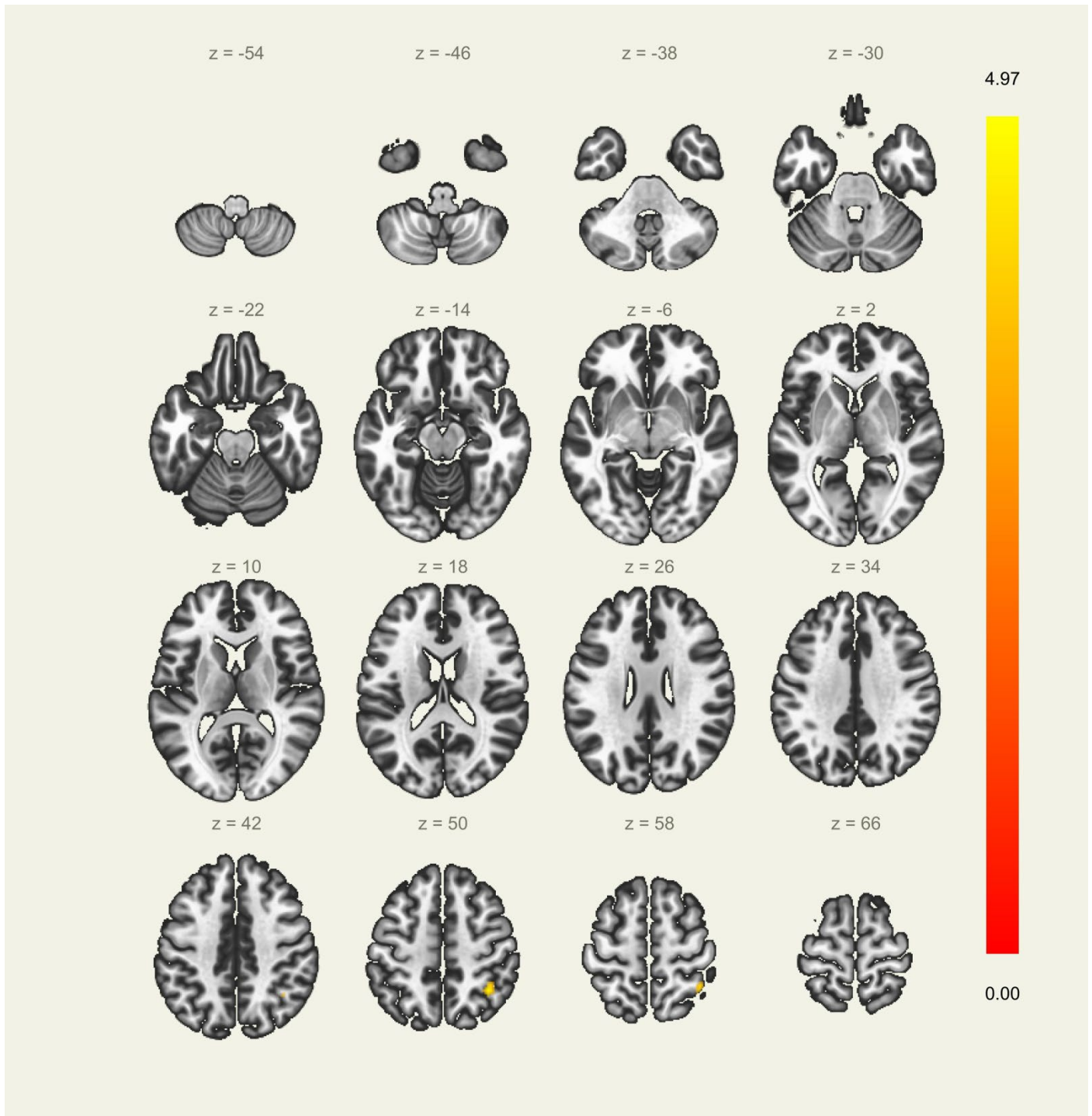
Online appendices are unedited and posted as supplied by the authors.



Supplemental figure 2. Seed-to-voxel analysis between low empathy vs. high empathy. Cluster +36 -50 +44, 136 voxels (69%) covering 9% of atlas right superior parietal lobule, indicated that the functional connectivity between anterior division of cingulate gyrus and right superior parietal lobule was relatively increased.

DOI: 10.1503/jpn240084

Online appendices are unedited and posted as supplied by the authors.



Supplemental figure 3. Seed-to-voxel analysis between low empathy vs. Healthy control. Cluster +38 -48 +54 , 119 voxels (88%) covering 8% of atlas right superior parietal lobule, and 16 voxels (12%) covering 1% of atlas right angular gyrus. What indicated that the functional connectivity between anterior division of cingulate gyrus and right superior parietal lobule was relatively increased.

Appendix 2 to Qu J-F, Liu X-W, Wang M-Z, et al. Structural-informed functional MRI analysis of patients with empathy impairment following stroke. *J Psychiatry Neurosci* 2024. Copyright © 2024 The Author(s) or their employer(s).
To receive this resource in an accessible format, please contact us at cmaigroup@cmaj.ca.

DOI: 10.1503/jpn240084

Online appendices are unedited and posted as supplied by the authors.